



Protective Effects of Xingnao Enema on Blood-brain Barrier Disruption in a Rat Model of Intracerebral Hemorrhage

Kun Wang^{1,2}, Yinglin Cui², Xu Zhao² and Changjiang Hu^{1*}

¹ Department of Pharmacy, Chengdu University of TCM, Chengdu 61137, China

² Department of the Second Clinical Medical College, Henan University of TCM, Zhengzhou 450002, China

ABSTRACT

Xingnao enema (XN) has been commonly used to treat intracerebral hemorrhage (ICH) in China with good therapeutic effect. As very little is known about the mechanism of action of XN, the purpose of this project was to investigate the neuroprotective effect of XN on ICH model rats and to explore the underlying mechanisms of this therapy. In this study, experimental ICH was induced by the administration of stereotaxic collagenase type VII into the caudate nucleus. XN (at a high dose and a low dose of 3.60g·kg⁻¹ and 1.80g·kg⁻¹, respectively) was administered via enema. The detection of neuronal apoptosis was measured by TUNEL assay. Using immunofluorescence, the expression of claudin-5, ZO-1 and VE-cadherin was detected. The expression of DNA methyltransferase 3b (DNMT3b) and Matrix metalloproteinase-9 (MMP-9) was evaluated by western blot. And microRNA-29b was identified using quantitative real-time PCR. 3). Compared with the Model group, the group treated with XN had a significantly reduced number of dead neurons in hippocampus and cortical regions of ICH rats. Furthermore, this treatment significantly increased protein expression of claudin-5, ZO-1 and VE-cadherin while protein expression of DNMT3b and MMP-9 were significantly inhibited. Finally, microRNA-29b level were also lower than the Model group. Our data suggests that XN has significant neuroprotective effects on the ICH model rats, which might help to protect the blood brain barrier by regulating of a cascade including the expression of microRNA-29b which regulates DNMT3b that in turn regulates level of MMP-9.

Article Information

Received 24 June 2019

Revised 06 July 2019

Accepted 11 July 2019

Available online 26 August 2019

Authors' Contribution

CYL, ZX and HCJ collaborated in the design of the study, contributed the reagents and materials and arranged the data. WK conducted the experiments, data analyses and wrote the manuscript.

Key words

Xingnao enema, Blood brain barrier, Intracerebral hemorrhage, Cerebral protection

INTRODUCTION

Intracerebral hemorrhage (ICH) is a disease with a complicated pathogenesis and high morbidity (Wilson *et al.*, 2014; Fiorella *et al.*, 2015). After ICH, hematoma, edema, secondary reaction including inflammatory reaction, oxidative stress and blood-brain barrier (BBB) damage can occur in succession (Ivanidze *et al.*, 2015). Disruption of the blood-brain barrier (BBB) plays an important role in the occurrence and development of ICH (Abbott *et al.*, 2006). Since the BBB can prevent some substances in the blood from entering the brain, it is commonly regarded as having a protective function between blood and the brain tissue (Ballabh *et al.*, 2004). The blood-brain barrier is mainly maintained by junction proteins such as claudins, zonula occludens and cadherins (Liu *et al.*, 2012). Studies have suggested that microRNA-29b regulates BBB dysfunction by regulating the level of

DNMT3b, which in turn regulating the level of MMP-9 (Kalani *et al.*, 2014), and MMP-9 can eat up the junction proteins such as claudin-5, ZO-1 and VE-cadherin and lead to leaky vasculature.

As a disease, ICH has attracted worldwide attention, however, effective therapies and drugs for this condition are still lacking. ICH is referred to as hemorrhagic apoplexy in Traditional Chinese Medicine (TCM). TCM has played a crucial role in the treatment of patients suffering from ICH. Specifically, the characteristics of multi-target and holistic treatment of TCM have shown some advantages in treating intracerebral hemorrhage through a complicated mechanism. In China, there are medical institutions that use Chinese herbal formula administered via enema to treat ICH patients; a process particularly suitable for coma patients.

Xingnao enema (XN) (Su *et al.*, 2014), a Chinese herbal formula including rhubarb, leech, *Acorus calamus* and borneol, has been prescribed to treat brain coma or brain injury patients after cerebral hemorrhage. Previous studies have shown that XN could shorten coma time, improve the permeability of the BBB and reduce the mortality and disability rate in patients with ICH (Zhang *et al.*, 2001;

* Corresponding author: hhccjj@hotmail.com
0030-9923/2019/0006-2233 \$ 9.00/0
Copyright 2019 Zoological Society of Pakistan

Cui *et al.*, 2000). However, the protective effect of XN on BBB integrity from a molecular standpoint requires further research. In this study, we explore on the protective effect of XN on BBB disruption following intracerebral hemorrhage in rats and the probable protective mechanism by which it acts.

MATERIALS AND METHODS

Materials

Male Wistar rats (250-300g) were provided by the Beijing Weitong Lihua Experimental Animal Technology Co., Ltd [License number: SCXK (jing):2016-0011]. The rats were housed in an environment that controlled temperature and humidity, and they could access to food and water freely. The weight of rats was monitored every day and all experiments were performed according to the procedures approved by Henan University of Traditional Chinese Medicine Animal Care and Use Committee.

Claudin 5 antibody was purchased from Lifespan and VE-cadherin-2 was obtained from Novus. ZO-1 antibody and MMP9 antibody were purchased from Proteintech Group Inc. (Wuhan, China). Finally, Dnmt3b antibody was purchased from Abcam (USA). Angong Niu Huang Pill was purchased from Beijing Tongrentang Technology Development Co., Ltd. (No: 1601 1928).

XN was provided by the Preparation Laboratory of Henan Province Hospital of Traditional Chinese Medicine. Drug preparation was as follows: (1) *Rhei radix et rhizoma* were extracted twice with ethanol for 1.5h each time: 10 times volume with ethanol was used for the first time and 8 times volume with ethanol was used for the second time. The two ethanol extracts were filtered and mixed and the tannins were removed with 5% gelatin. At last the extracts were concentrated to 1.5g·ml⁻¹. (2) *Hirudo nipponica Whitman* was digested two times (2h each time) in room temperature water. The extract was filtered, mixed and vacuum condensed to concentration of 0.9g·ml⁻¹. (3) The volatile oil of *Acorus tatarinowii Schott* was extracted via water vapor distillation. (4) *L-borneolum* was crushed into fine powder. Subsequently, *Rhei radix et rhizoma* and *Hirudo nipponica Whitman* extractions, *Acorus tatarinowii Schott* volatile Oil and *L-borneolum* fine powder were mixed and the concentration was adjusted to 1.5g/crude herb/ml with 0.5g·ml⁻¹ carboxymethylcellulose sodium (CMC).

Angong Niu Huang pill (AGNH) was prepared into 0.18g·ml⁻¹ suspension with 0.5g·ml⁻¹ CMC.

Establishment of rat model

XN (at a high dose and low dose of 3.6g·kg⁻¹ and 1.8g·kg⁻¹, respectively) was administered via enema to

rats for one week prior to ICH induction. Besides control group, rats were anesthetized with 4% chloral hydrate intraperitoneally (8 mL·kg⁻¹). Using a stereoscopic locator, a longitudinal incision about 1cm was made at the midline of scalp, with a deviation to right of about 3mm. Then, scalp and subcutaneous tissue was separated, and a blunt separation was made in the periosteum. According to the position of the anterior fontanelle, the position of 2mm at the front of the front fontanelle and middle line was opened 3mm, and a hole about 1mm in diameter was drilled using a dental drill. A microinjector was used to inject vertically along the borehole direction with the depth of 4.0 mm, and then 0.5μl collagenase VII was injected into the caudate nucleus slowly and equally. The whole injection process was controlled within 3 minutes. After the injection, the needle was kept for 10 minutes, and slowly withdrew from the microinjector. Finally, the sewn skin was sutured after slow withdrawal of the needle and each animal was placed in an empty cage for recovery. During the surgical period, the body temperature of animals was maintained using an electric lamp irradiation.

Longa 5 grade scoring method was used to evaluate the success in establishing the ICH rat model. In total, 48 successful wistar rats were randomly divided into four groups: Angong Niu Huang pill group, high-dose XN group and low-dose XN group, model group; in addition, designed blank group and sham operation group, 6 rats in each group. Each group was respectively given Angong Niu Huang pill (0.27 g·kg⁻¹), high-dose XN (3.60 g·kg⁻¹) and low-dose XN (1.80 g·kg⁻¹), normal saline, normal saline and normal saline through enema for 3 days (once a day) before establishment of ICH model. After successful establishing the model, the drug was continually given for 3 days. After the last administration, the caudal venous serum was taken from each rat for 2 mL; Six rats in each group were treated with paraffin section of the hemorrhage side brain tissue, and the remaining 6 rats were extracted the total protein from the hemorrhage side brain tissue.

Drug administration and sample collection

After ICH model rat recovery, 1.80g·kg⁻¹ XN was administered by enema for the low-dose XN group, 3.60g·kg⁻¹ XN was administered by enema for the high-dose XN group and 0.27g·kg⁻¹ AGNH was administered by enema for positive group. The blank control group, Model group and Sham control group were injected with the same amount of normal saline. All of this administration occurred in one day.

Rats were anesthetized with 4% chloral hydrate (8 mL·kg⁻¹) and sacrificed three days after ICH induction. Brain tissue was removed and cleaned with PBS. Brain tissue samples were frozen at -80°C for western blot and

quantitative real-time PCR experiments. Some brain tissue samples were soaked in 4% paraformaldehyde at 4°C for further immunohistochemistry experimentation.

TUNEL assay

The cerebral tissues of ICH rats were fixed with 4% paraformaldehyde (8:1) for 24 h. According to the instructions of apoptosis detection kit, the cerebral tissues were dehydrated by series of elevated ethanol concentrations, embedded in paraffin wax, sliced and dewaxed. After rinsing in PBS, each sample was incubated with 20 $\mu\text{g}\cdot\text{mL}^{-1}$ proteinase K solution at the room temperature for 20 min and then washed again with PBS. Each sample was then incubated with Equilibrium Buffer-dUTP-TdT Enzyme (10:5:1) at the room temperature for 30 min. DAPI solution was used to dye the nucleus and the reaction was protected from light for 5 min. Then the film was sealed with sealing liquid containing a fluorescence quenching agent, and the results were observed under the fluorescence microscope.

The apoptotic cells had green fluorescence and the nuclei had blue fluorescence within tissue sections. Using the conventional labeling index, three high-power visual fields (400x) were selected and each cell was counted. Finally the labeling index of each field was counted. Labeling index was defined as the number of positive cells in each field / all cells in the field. The apoptotic index of each case was equal to the average of the labeling indexes for each field.

Immunohistochemistry analysis

Cortex and hippocampal hemorrhage side brain tissues were fixed with paraformaldehyde (8:1,V/V) and then were dehydrated in an ascending alcohol series, embedded with paraffin and then sectioned. After the sections were deparaffinized and rehydrated, the sections were quenched in the 3% hydrogen peroxide and methanol solution, then blocked in the normal goat serum for 30 min at the room temperature. Furthermore, antibody claudin-5, ZO-1 and VE-cadherin diluted with PBS (1:200, 1:100, 1:200, respectively) were added. While the sections were incubated overnight at 4°C, rinsed with PBS, dried with absorbent paper. Then the secondary antibody (HRP-labeled goat anti-rabbit) was added dropwise, incubated for 20 min at the room temperature, washed with PBS, and dried with absorbent paper. Freshly prepared DAB chromogen was added to each section and observed under a microscope. After the color development was completed, the sections were washed with tap water to terminate the color development, Harris hematoxylin was counter-dyed, dehydrated, seal the slice. Finally, the images were observed and collected under the microscope.

Western blot analysis

The expression of DNMT3b and MMP-9 protein was assessed by western blot. The total protein of hemorrhage side brain tissues was extracted and measured using the Bradford method. Equal amounts of protein (40 μg) were denatured by boiling for 10min, separated with SDS-PAGE electrophoresis and then transferred to the PVDF membranes. After that, the PVDF membranes were blocked with blocking buffer TBST containing 5% skimmed milk powder for 2h at the room temperature. Then the membrane were incubated with primary antibodies overnight at 4°C, and followed with the secondary antibody incubation at the room temperature for 2h. The PVDF membranes were washed by TBST for 6 times (5 min each time). The enhancement solution in ECL reagent was mixed with the stable peroxidase solution at 1:1, and the working solution was added to the PVDF membranes. After the reaction to the obvious fluorescence band, the excess substrate was absorbed by filter paper and the plastic wrap was covered. Then the X-ray film is pressed into the developing solution, fixative solution in turn and the film is developed. Dry and scan the film and analyze the gray value of the film with BandScan 5.0 software. The relative expression level of the protein is expressed by the gray value of the target protein/GAPDH gray value.

Quantitative real-time PCR for microRNA-29b

First, total RNA was extracted from the samples. Differential spectrophotometry (OD260/280) was used to determine the purity and integrity of the total RNA. Then the reverse-transcription reactions were performed using a Hiscrypt Reverse Transcriptase kit. Quantitative real-time PCR was prepared using the SYBR Green dye method. In the end, a dissolution curve was drawn and the relative expression level of microRNA-29b was calculated with $2^{-\Delta\Delta\text{Ct}}$.

Statistical analysis

Statistical analysis was analyzed in SPSS 18.0 software using one-way ANOVA analysis. All values were presented as means \pm SEM. $P < 0.05$ was used to indicate a statistical significance.

RESULTS

Neuronal apoptosis in ICH rats

The index of neuronal apoptosis in the model group were significantly more than the sham-operated group. The neuronal apoptosis in the blank group and the sham-operated group were rarely detected in the tissues surrounding the bleeding site, indicating that the ICH model is successful. After XN intervention, the index of

neuronal apoptosis in the low-dose and high-dose XN enema groups were reduced significantly compared with the model group (** $P < 0.01$; Table I, Fig. 1).

Table I.- Effect of XN on neuronal apoptosis in hemorrhagic brain tissue in ICH rats ($\bar{x} \pm s$; n=6).

Group	Dosage	Apoptotic index (%)
Blank group	-	0.88 ± 0.14
Sham-operated group	-	12.49 ± 6.36
Model group	-	43.26 ± 6.55 ^{##}
AGNH group	0.27g · kg ⁻¹	6.57 ± 1.82 ^{**}
XN (low dose)	1.80g · kg ⁻¹	23.82 ± 3.89 ^{**}
XN (high dose)	3.60g · kg ⁻¹	13.05 ± 1.42 ^{**}

[#] $P < 0.05$, ^{##} $P < 0.01$, versus sham-operated group; ^{*} $P < 0.05$, ^{**} $P < 0.01$, versus model group

Expression of claudin-5, ZO-1 and VE-cadherin-2 in ICH rats

Compared with the sham-operated group, the expression of claudin-5, VE-Cadherin-2, and ZO-1 protein in the hippocampus and cortical regions of model group was significantly lower (^{##} $P < 0.01$). The results showed that 3 days after ICH model induction the integrity of BBB was destroyed. Protein expression of AGNH group was higher than those of the ICH group. After XN enema intervention,

the protein expression levels in the hippocampus regions of the XN-high dose group were higher than those of the model group (claudin-5, ^{**} $P < 0.01$; ZO-1, ^{**} $P < 0.01$; VE-cadherin, ^{*} $P < 0.05$), in the cortical regions higher than those of the model group too (Claudin-5, ^{**} $P < 0.01$; ZO-1, ^{**} $P < 0.01$; VE-cadherin, ^{**} $P < 0.01$). The expression levels of Claudin-5, ZO-1, VE-Cadherin-2 protein in the

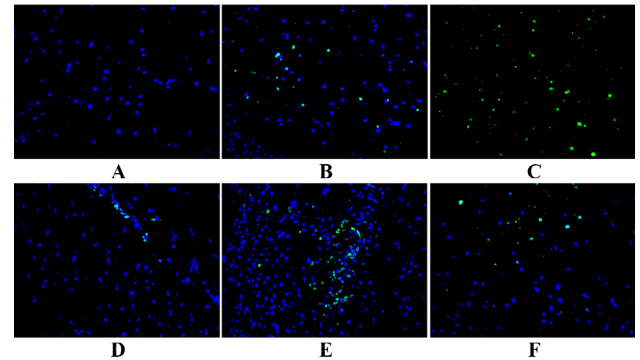


Fig. 1. Effect of XN on neuronal apoptosis in hemorrhagic brain tissue of ICH rats. Under the fluorescence microscope, blue represents cell nuclei, green intensity represents apoptotic cells in the blank group (A), sham-operated group (B), model group (C), AGNH group (D) and XN-treated (low/high doses, E/F) groups. The two patterns were superimposed to determine the apoptosis. All images were taken at 400× magnification.

Table II.- Effect of XNE on the expression of Claudin-5, ZO-1 and VE-cadherin protein in hippocampus and cortical regions of ICH rats ($\bar{x} \pm s$; n=6).

Group	Dosage	Density		
		Claudin-5	ZO-1	VE-cadherin
Hippocampus				
Blank group	-	0.0106 ± 0.0008	0.0074 ± 0.0007	0.0143 ± 0.0020
Sham-operated group	-	0.0070 ± 0.0007	0.0180 ± 0.0020	0.0185 ± 0.0033
Model group	-	0.0017 ± 0.0001 ^{##}	0.0027 ± 0.0004 ^{##}	0.0084 ± 0.0009 ^{##}
AGNH group	0.27g · kg ⁻¹	0.0052 ± 0.0003 [*]	0.0145 ± 0.0012 ^{**}	0.0161 ± 0.0012 ^{**}
XN (low dose)	1.80g · kg ⁻¹	0.0038 ± 0.0001	0.0060 ± 0.0009 [*]	0.0095 ± 0.0013
XN (high dose)	3.60g · kg ⁻¹	0.0073 ± 0.0019 ^{**}	0.0085 ± 0.0005 ^{**}	0.0134 ± 0.0016 [*]
Cortical regions				
Sham-operated group	-	0.0054 ± 0.0008	0.0101 ± 0.0003	0.0221 ± 0.0013
Model group	-	0.0016 ± 0.0001 ^{##}	0.0028 ± 0.0007 ^{##}	0.0061 ± 0.0007 ^{##}
AGNH group	0.27g · kg ⁻¹	0.0051 ± 0.0009 ^{**}	0.0089 ± 0.0005 ^{**}	0.0144 ± 0.0007 ^{**}
XN (low dose)	1.80g · kg ⁻¹	0.0021 ± 0.0002	0.0037 ± 0.0006	0.0076 ± 0.0014
XN (high dose)	3.60g · kg ⁻¹	0.0074 ± 0.0006 ^{**}	0.0064 ± 0.0006 ^{**}	0.0124 ± 0.0009 ^{**}

For details, see Table I.

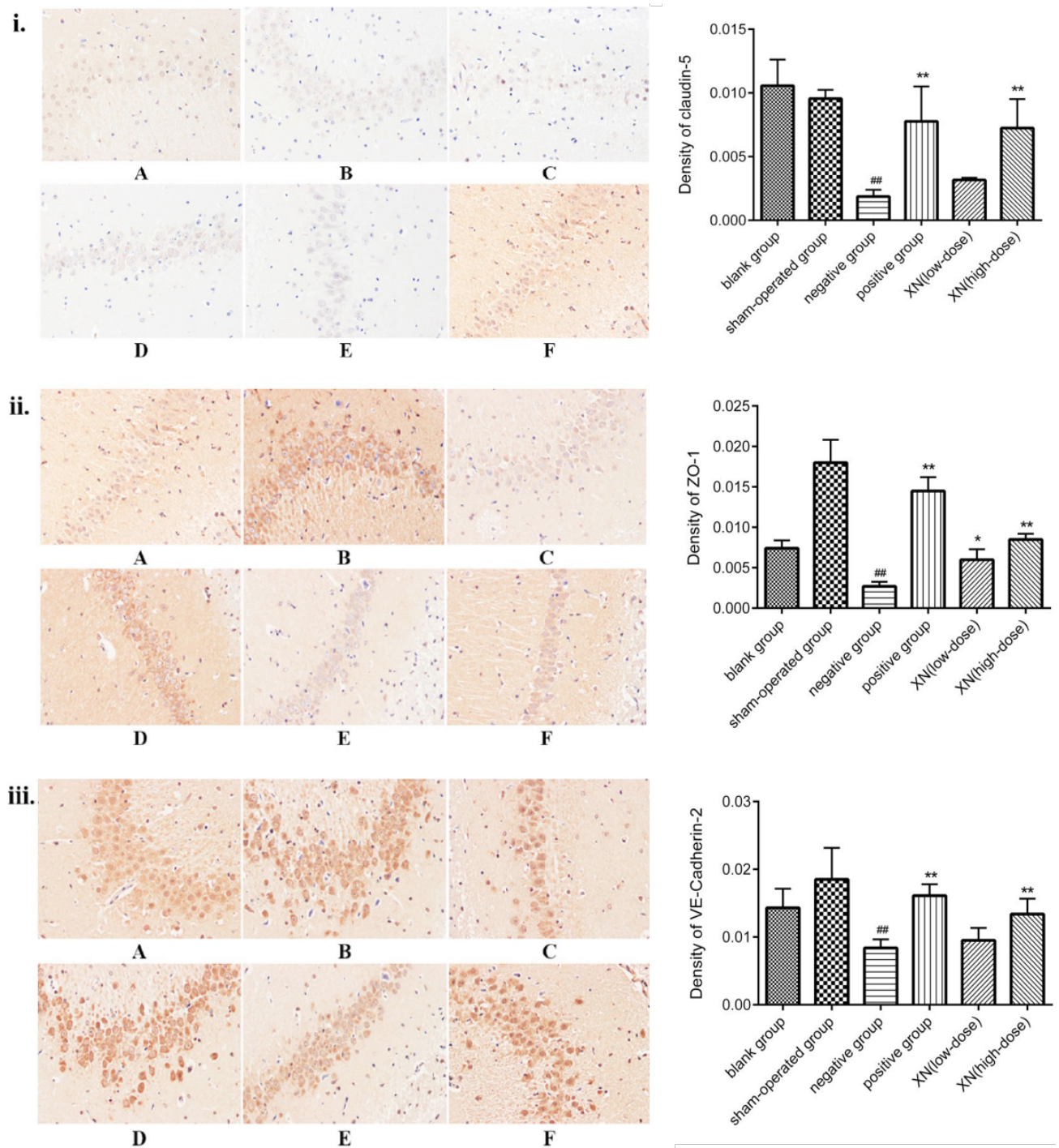


Fig. 2. Expression alteration of claudin-5, ZO-1 and VE-cadherin protein by immunohistochemistry in ICH rat hippocampus tissue in blank group (A), sham-operated group (B), model group (C), AGNH group (D), and XN-treated (low/high doses, E/F) groups. All images were taken at 400 \times magnification. (i) expression of Claudin-5 protein in hippocampus of ICH rats; (ii) expression of ZO-1 protein in hippocampus of ICH rats; (iii) expression of VE-cadherin protein in hippocampus of ICH rats. The results are also expressed in a bar graph showing the density alteration of claudin-5, ZO-1 and VE-cadherin protein in hippocampal tissue. Data are represented as mean \pm SEM ($\#P<0.05$, $\#\#P<0.01$, versus sham-operated group; $*P<0.05$, $**P<0.01$, versus model group); data analyzed from six independent experiments (n=6).

Table III: Effect of XN on the expression of MMP-9 and DNMT3b in ICH rats ($\bar{x}\pm s$; n=6).

Group	Dosage	MMP-9/GAPDH	DNMT3b/GAPDH
Blank group	-	0.3795 \pm 0.084	0.363 \pm 0.0240
Sham-operated group	-	0.3935 \pm 0.056	0.380 \pm 0.0255
Model group	-	0.8305 \pm 0.135 ^{##}	0.632 \pm 0.0453 ^{##}
AGNH group	0.27g·kg ⁻¹	0.5880 \pm 0.023*	0.433 \pm 0.0042**
XN (low dose)	1.80g·kg ⁻¹	0.7440 \pm 0.052	0.557 \pm 0.0361*
XN (high dose)	3.60g·kg ⁻¹	0.6030 \pm 0.004*	0.497 \pm 0.0021**

For details, see Table I.

hippocampus regions of XN-low dose group were higher than those of the model group, but there is no significant difference ($P>0.05$) except ZO-1 ($*P<0.05$); in cortical regions higher than those of the model group, but there is no significant difference either ($P>0.05$) (Table II, Figs. 2-3).

Expression of MMP-9 and DNMT3b in ICH rats

Compared with the sham-operated group, the expression levels of MMP-9/GAPDH and DNMT3b/GAPDH in the model group were significantly (^{##} $P<0.01$) elevated; compared with the model group, the expression levels of MMP-9/GAPDH and DNMT3b/GAPDH in high-dose XN group were significantly alleviated (MMP-9/GAPDH, $*P<0.05$; DNMT3b/GAPDH, $**P<0.01$), the expression levels of MMP-9/GAPDH and DNMT3b/GAPDH in low-dose XN group were alleviated (MMP-9/GAPDH, no significant difference, $P>0.05$; DNMT3b/GAPDH, $*P<0.05$) (Table III, Fig. 4).

Level of microRNA-29b in ICH rats

Compared with the sham-operated group, the expression of microRNA-29b increased in model group (^{##} $P<0.01$). Compared with the model group, the microRNA-29b level significantly decreased in XN-high dose group ($**P<0.01$), and there is no significant difference in XN-low dose group ($P>0.05$) (Table IV, Fig. 5).

DISCUSSION

TCM has played a crucial role in the treatment of ICH. Zheng *et al.* (2014) used the Marmarou method to make diffuse brain injury model in rats. It was found that the Angong Niuhuang pill, a TCM preparation, could effectively protect the BBB and brain tissue, and significantly reduce edema, cerebral infarct size, and cell apoptosis. Our previous studies have been preliminary

studies on the protective effect of XN by clinical and pharmacological experiments (Cui *et al.*, 2000). Cui Yinglin *et al.* used XN in the ICH rat model and found that XN could promote the absorption of hematoma and has a better effect in reducing intracranial pressure. Clinically, XN has been used by Cui Yinglin in coma patients with intracerebral hemorrhage and found that it alleviated brain edema, relieved intracranial pressure and improved the permeability of the BBB. As a consequence, maintaining the integrity of the BBB is very important for brain protection after ICH.

Table IV: Effect of XN on the expression of microRNA-29b in ICH rats ($\bar{x}\pm s$; n=6).

Group	Dosage	MicroRNA-29b
Blank group	-	0.984 \pm 0.300
Sham-operated group	-	0.895 \pm 0.248
Model group	-	2.482 \pm 0.512 ^{##}
AGNH group	0.27g·kg ⁻¹	1.552 \pm 0.334**
XN (low dose)	1.80g·kg ⁻¹	2.135 \pm 0.359
XN (high dose)	3.60g·kg ⁻¹	1.802 \pm 0.534**

For details, see Table I.

BBB is a unique barrier structure of brain microvessels which can selectively penetrate substances and can prevent harmful substances from entering the brain tissue, thereby it can maintain the stability of the CNS environment in the central nervous system (Ivanidze *et al.*, 2015). The pathological mechanism of brain injury after ICH is very complicated. After ICH, the permeability of BBB around hematoma is enhanced, resulting in the destruction of the physiological function of BBB-mediated substance transmission, which in turn leads to vasogenic brain edema around the hematoma (Shiba *et al.*, 2014; Han *et al.*, 2008). Meanwhile, various cytotoxic substances produced by ICH

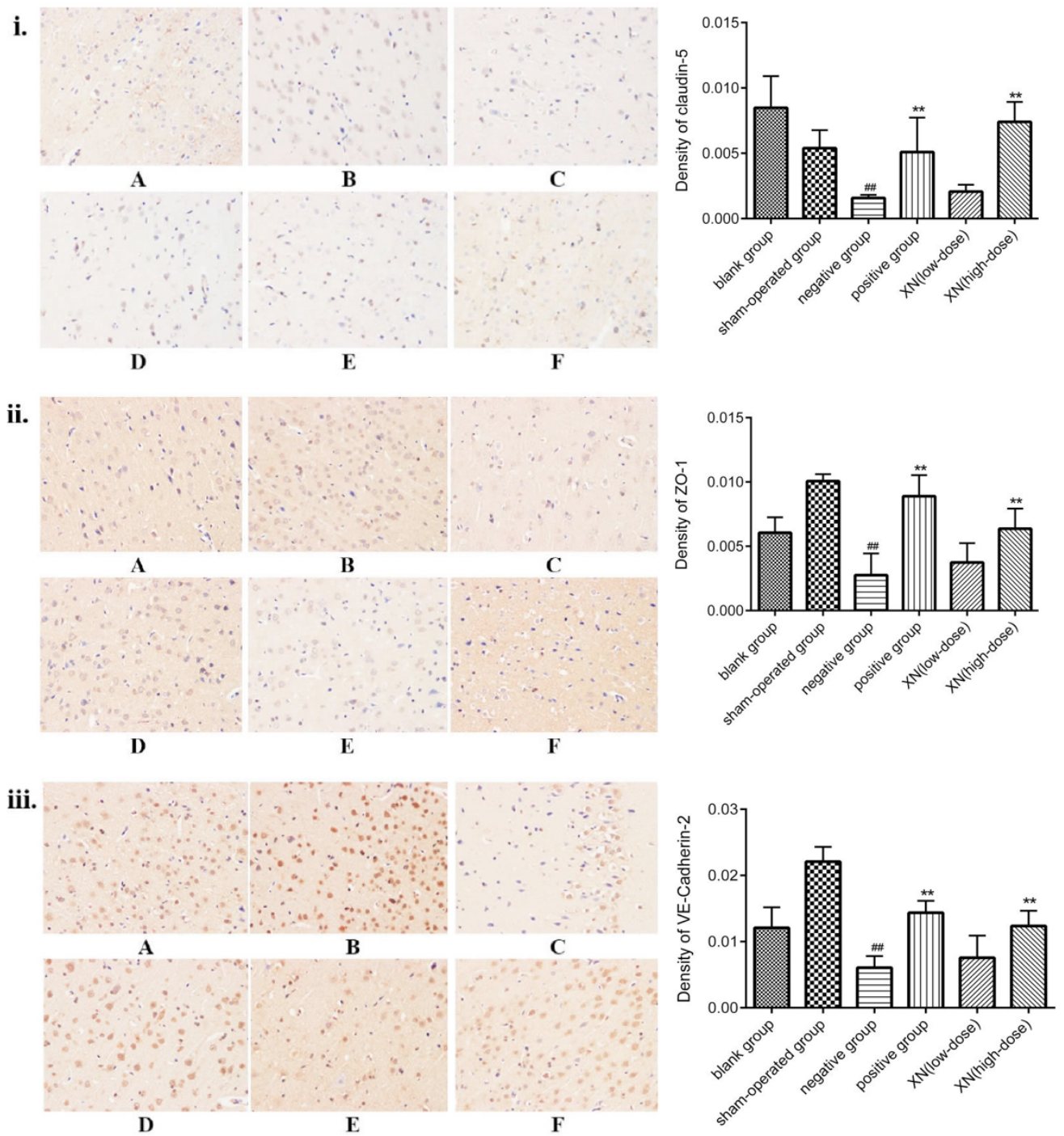


Fig. 3. Expression alteration of claudin-5, ZO-1 and VE-cadherin protein by immunohistochemistry in ICH rat cortical regions in blank group (A), sham-operated group (B), model group (C), AGNH group (D), and XN-treated (low/high doses, E/F) groups. All images were taken at 400 \times magnification. (i) expression of claudin-5 protein in cortical regions of ICH rats; (ii) expression of ZO-1 protein in cortical regions of ICH rats; (iii) expression of VE-cadherin protein in cortical regions of ICH rats. The results are also expressed in bar graph showing density alteration of claudin-5, ZO-1 and VE-cadherin protein in cortical regions. Data represented as mean \pm SEM ([#] P <0.05, ^{##} P <0.01, versus sham-operated group; ^{*} P <0.05, ^{**} P <0.01, versus model group); data analyzed from six independent experiments (n=6).

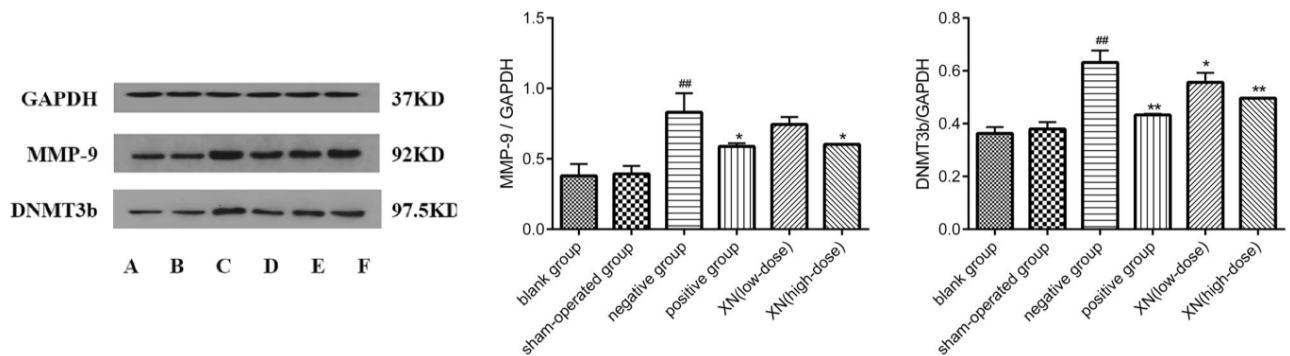


Fig. 4. SDS-PAGE effect of XN on the expression of MMP-9 and DNMT3b in ICH rats. Western blot results showed expressions of MMP-9 and DNMT3b in blank group(A), sham-operated group (B), model group (C), AGNH group (D), and XN-treated (low/high doses, E/F) groups. Protein expressions are normalized with their respective glyceraldehyde 3-phosphate dehydrogenase (GAPDH) controls and the results are also represented in a bar graph showing MMP9 and DNMT3b band intensity, normalized with GAPDH band intensity. Data represent mean \pm SEM (# P <0.05, ## P <0.01, versus sham-operated group; * P <0.05, ** P <0.01, versus model group); data analyzed from six independent experiments (n=6).

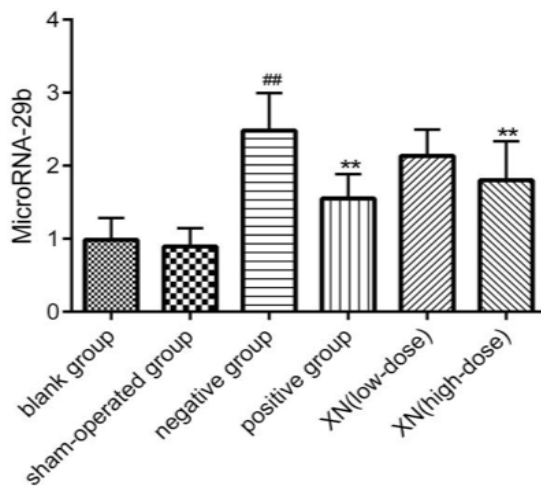


Fig. 5. The effect of XN on the expression of microRNA-29b in ICH rats. Bar graph showing the change in microRNA-29b protein expression in the blank, sham-operated, model, AGNH group and XN-treated (low/high doses) groups. Data represented as mean \pm SEM (# P <0.05, ## P <0.01, versus sham-operated group; * P <0.05, ** P <0.01, versus model group); data analyzed using six independent experiments (n=6).

can lead to necrosis and apoptosis of nerve cells after moving through the BBB (Ansar *et al.*, 2014; Zhang *et al.*, 2003). Many animal experiments and clinical researches have confirmed that destruction of the BBB is a common and important pathophysiological change after cerebral hemorrhage (El Amki *et al.*, 2018; Wang *et al.*, 2012). In our study, the ICH rat model was established, and it was found that the apoptotic index of the brain

tissue in the hemorrhagic side and its surrounding tissues increased significantly (P <0.01) (as shown in Fig.1), which indicated that the breakdown of the BBB after intracerebral hemorrhage further led to the apoptosis of nerve cells. Therefore, maintaining the integrity of the BBB may be a potential therapeutic target for ICH and other brain microvascular injury related diseases.

Matrix metalloproteinases (MMPs) are a group of proteolysis enzymes that can degrade extracellular matrix including neurovascular basement membrane and tight junction of proteins in BBB (Akpınar *et al.*, 2016; Chou *et al.*, 2011). Within the subtypes of MMPs, MMP-9 is thought to be closely related to the BBB injury induced by cerebral ischemia-reperfusion injury (Rottenberger and Kolev, 2011). Among the structural protein that form the BBB, Claudin-5 and ZO-1 are important tight junction protein, and VE-cadherin is an important adhesion protein. And the expression of these protein is crucial for maintaining the integrity of the BBB (Chen *et al.*, 2012; Yang *et al.*, 2007). Evidence has indicated that during cerebral ischemia, the expression of MMP-9 increased significantly in the vascular endothelial cells of cerebral infarction and surrounding lesions. MMP-9 can increase BBB permeability by breaking down tight junction protein during cerebral ischemia, which plays the key role in the formation of cerebral edema (Kumar and Patnaik, 2017; Zhu *et al.*, 2015). Considering our research, as shown in Figure 2-3, the expression of claudin-5, ZO-1 and VE-cadherin protein in hippocampus and cortical brain of the hemorrhage side decreased significantly after intracerebral hemorrhage (P <0.01). Therefore, drugs that can regulate the expression of MMP-9 may be effective in ICH brain protection. Guo *et al.* (Guo *et al.*, 2011) and Suzuki *et al.*

(Suzuki *et al.*, 2011) showed that inhibition of MMP-9 can reduce early brain damage after subarachnoid hemorrhage in rats. Anuradha Kalani *et al.* (Kalani *et al.*, 2014) also confirmed that microRNA-29b can directly target DNA methyltransferase 3b (DNMT3b). DNMT3b can target MMP-9, then MMP-9 can break the tight junction protein and cause the increase of BBB permeability (Garzon *et al.*, 2009; Fabbri *et al.*, 2007). Thus, the regulation of microRNA-29b on the DNMT3b/MMP-9 pathway has been well established (Khanna *et al.*, 2013; Kalani *et al.*, 2013). Moreover, our data also confirmed that the expression of microRNA-29b, DNMT3b and MMP-9 in the brain tissue of the hemorrhagic side of the ICH rat model was increased (Fig. 4, 5), indicating that the pathway of microRNA-29b/DNMT3b/MMP-9 was stimulated leading to the destruction of the BBB and the apoptosis of nerve cells. Therefore, a future direction in drug research for brain protection in patients with ICH should focus on those that interfere with the expression of microRNA-29b.

The aim of this study was to provide a new approach to predict whether XN could maintain the integrity of the BBB by regulating the microRNA-29b/DNMT3b/MMP-9 pathway. Our results suggested that the expression of claudin-5, ZO-1 and VE-cadherin proteins, which are related to the BBB in hippocampus and cortical regions of ICH rats, was increased after interference by XN (Fig. 2, 3). Neuronal apoptosis was also decreased (Table 1) indicating that XN may play a cerebral protective effect by maintaining the integrity of the BBB. Our results also confirmed that XN enema could decrease the expression of microRNA-29b, DNMT3b and MMP-9 (Fig. 4, 5). In other words, there was a negative correlation between XN treatment and microRNA-29b /DNMT3b /MMP-9 pathway, indicating that the XN enema could maintain the integrity of the BBB in ICH rats by regulating microRNA-29b/DNMT3b/MMP-9 pathway and further exerting brain protection.

CONCLUSIONS

Our results demonstrate that XN could reduce the apoptosis of nerve cells, stimulate the expression of claudin 5, ZO-1 and VE-cadherin and inhibit the expression of microRNA-29b, DNMT3b and MMP-9. In summary, XN has a protective effect on the BBB disruption following intracerebral hemorrhage. Furthermore these results may provide some theoretical basis for future research on microRNA-29b expression in ICH patients.

ACKNOWLEDGEMENT

We acknowledge the financial supports of the National

Natural Science Foundation of China under Grant No. 8157150811. The authors give their sincere appreciation to the researchers in the central lab of the Second Clinical Medical College, Henan University of Traditional Chinese Medicine for their selfless help.

Statement of conflict of interest

We declare no conflicts of interest in this study.

REFERENCES

- Abbott, N.J., Ronnback, L. and Hansson, E., 2006. Astrocyte-endothelial interactions at the blood-brain barrier. *Nat. Rev. Neurosci.*, **7**: 41-53. <https://doi.org/10.1038/nrn1824>
- Akpinar, A., Ucler, N., Erdogan, U., Baydin, S.S., Gungor, A. and Tugcu, B., 2016. Measuring serum matrix metalloproteinase-9 level in peripheral blood after subarachnoid hemorrhage to predict cerebral vasospasm. *SpringerPlus*, **5**: 1153. <https://doi.org/10.1186/s40064-016-2837-6>
- Ansar, S., Chatzikonstantinou, E., Thiagarajah, R., Tritschler, L., Fatar, M., Hennerici, M.G. and Meairs, S., 2014. Proinflammatory mediators and apoptosis correlate to rt-PA response in anovel mousemodel of thromboembolic stroke. *PLoS One*, **8**: e85849. <https://doi.org/10.1371/journal.pone.0085849>
- Ballabh, P., Braun, A. and Nedergaard, M., 2004. The blood-brain barrier: an overview: structure, regulation, and clinical implications. *Neurobiol. Dis.*, **16**: 1-13. <https://doi.org/10.1016/j.nbd.2003.12.016>
- Chen, D., Wei, X.T., Guan, J.H., Yuan, J.W., Peng, Y.T., Song, L. and Liu, Y.H., 2012. Inhibition of c-Jun N-terminal kinase prevents blood-brain barrier disruption and normalizes the expression of tight junction proteins claudin-5 and ZO-1 in a rat model of subarachnoid hemorrhage. *Acta Neurochir.*, **154**: 1469-1476. <https://doi.org/10.1007/s00701-012-1328-y>
- Chou, S.H., Feske, S.K., Simmons, S.L., Konigsberg, R.G., Orzell, S.C., Marckmann, A., Bourget, G., Bauer, D.J., De Jager, P.L., Du, R., Arai, K., Lo, E.H. and Ning, M.M., 2011. Elevated peripheral neutrophils and matrix metalloproteinase 9 as biomarkers of functional outcome following subarachnoid hemorrhage. *Transl. Stroke Res.*, **4**: 600-607. <https://doi.org/10.1007/s12975-011-0117-x>
- Cui, Y.L., 2000. Clinical observation on treatment of acute cerebral hemorrhagic coma by xingnao

- enema solution. *Liaoning J. Tradit. Chin. Med.*, **27**: 364-365.
- El Amki, M., Dubois, M., Lefevre-Scelles, A., Magne, N., Roussel, M., Clavier, T., Guichet, P.O., Gérardin, E., Compère, V. and Castel, H., 2018. Long-lasting cerebral vasospasm, microthrombosis, apoptosis and paravascular alterations associated with neurological deficits in a mouse model of subarachnoid hemorrhage. *Mol. Neurobiol.*, **55**: 2763-2779. <https://doi.org/10.1007/s12035-017-0514-6>
- Fabbri, M., Garzon, R., Cimmino, A., Liu, Z., Zanesi, N., Callegari, E., Liu, S., Alder, H., Costinean, S., Fernandez-Cymering, C., Volinia, S., Guler, G., Morrison, C.D., Chan, K.K., Marcucci, G., Calin, G.A., Huebner, K. and Croce, C.M., 2007. MicroRNA-29 family reverts aberrant methylation in lung cancer by targeting DNA methyltransferases 3A and 3B. *Proc. natl. Acad. Sci. U.S.A.*, **104**: 15805-15810. <https://doi.org/10.1073/pnas.0707628104>
- Fiorella, D., Zuckerman, S.L. and Khan, I.S., Ganesh, Kumar, N. and Mocco, J., 2015. Intracerebral Hemorrhage: A common and devastating disease in need of better treatment. *World Neurosurg.*, **84**: 1136-1141. <https://doi.org/10.1016/j.wneu.2015.05.063>
- Garzon, R., Liu, S., Fabbri, M., Liu, Z., Heaphy, C.E., Callegari, E., Schwind, S., Pang, J. and Yu, J., 2009. MicroRNA-29b induces global DNA hypomethylation and tumor suppressor gene re-expression in acute myeloid leukemia by targeting directly DNMT3A and 3B and indirectly DNMT1. *Blood*, **113**: 6411-6418. <https://doi.org/10.1182/blood-2008-07-170589>
- Guo, Z.D., Zhang, X.D., Wu, H.T., Lin, B., Sun, X.C. and Zhang, J.H., 2011. Metalloproteinase 9 inhibition reduces early brain injury in cortex after subarachnoid hemorrhage. *Acta Neurochir. Suppl.*, **110**: 81-84. https://doi.org/10.1007/978-3-7091-0353-1_15
- Han, N., Ding, S.J., Wu, T., Zhu, Y.L., 2008. Correlation of free radical level and apoptosis after intracerebral hemorrhage in rats. *Neurosci. Bull.*, **24**: 351-358.
- Ivanidze, J., Kesavabhotla, K., Kallas, O.N., Mir, D., Baradaran, H., Gupta, A., Segal, A.Z., Claassen, J. and Sanelli, P.C., 2015. Evaluating blood-brain barrier permeability in delayed cerebral infarction after aneurysmal subarachnoid hemorrhage. *Am. J. Neuroradiol.*, **36**: 850-854. <https://doi.org/10.3174/ajnr.A4207>
- Kalani, A., Kamat, P.K., Tyagi, S.C. and Tyagi, N., 2013. Synergy of homocysteine, microRNA and epigenetics: A novel therapeutic approach for stroke. *Mol. Neurobiol.*, **48**: 157-168. <https://doi.org/10.1007/s12035-013-8421-y>
- Kalani, A., Kamat, P.K., Familtseva, A., Chaturvedi, P., Muradashvili, N., Narayanan, N., Tyagi, S.C. and Tyagi, N., 2014. Role of microRNA29b in blood-brain barrier dysfunction during hyperhomocysteinemia: an epigenetic mechanism. *J. Cereb. Blood Flow Metab.*, **34**: 1212-1222. <https://doi.org/10.1038/jcbfm.2014.74>
- Khanna, S., Rink, C., Ghoorkhanian, R., Gnyawali, S., Heigel, M., Wijesinghe, D.S., Chalfat, C.E., Chan, Y.C., Banerjee, J., Huang, Y., Roy, S. and Sen, C.K., 2013. Loss of miR-29b following acute ischemic stroke contributes to neural cell death and infarct size. *J. Cereb. Blood Flow Metab.*, **33**: 1197-1206. <https://doi.org/10.1038/jcbfm.2013.68>
- Kumar, G. and Patnaik, R., 2017. Inhibition of gelatinases (MMP-2 and MMP-9) by *Withania somnifera* phytochemicals confers neuroprotection in stroke: An in-silico analysis. *Interdiscip. S.C.I.*, **10**: 1-12. <https://doi.org/10.1007/s12539-017-0231-x>
- Liu W.Y., Wang Z.B., Zhang L.C., Wei X. and Li, L., 2012. Tight junction in blood-brain barrier: an overview of structure, regulation, and regulator substances. *CNS Neurosci. Ther.*, **18**: 609-615. <https://doi.org/10.1111/j.1755-5949.2012.00340.x>
- Naidech, A.M., 2015. Diagnosis and management of spontaneous intracerebral hemorrhage. *Continuum (Minneap. Minn.)*, **12**: 1288-1298. <https://doi.org/10.1212/CON.0000000000000222>
- Rottenberger, Z., Kolev, K., 2011. Matrix metalloproteinases at key junctions in the pathomechanism of stroke. *Cent. Eur. J. Biol.*, **6**: 471-485. <https://doi.org/10.2478/s11535-011-0030-z>
- Shiba, M., Fujimoto, M., Imanaka-Yoshida, K., Yoshida, T., Taki, W. and Suzuki, H., 2014. Tenascin-C causes neuronal apoptosis after subarachnoid hemorrhage in rats. *Transl. Stroke Res.*, **5**: 238-247. <https://doi.org/10.1007/s12975-014-0333-2>
- Suzuki, H., Ayer, R., Sugawara, T., Chen, W., Sozen, T., Hasegawa, Y., Kanamaru, K. and Zhang, J.H., 2011. Role of osteopontin in early brain injury after subarachnoid hemorrhage in rats. *Acta Neurochir Suppl.*, **110**: 75-79. https://doi.org/10.1007/978-3-7091-0353-1_14
- Su, X.P., Wang, D.C., Zhang, R., Chen, X.M. and Zhu, X.F., 2014. Effect of xingnao enema solution in stroke coma. *J. Emerg. Tradit. Chin. Med.*, **23**:

- 334-335.
- Wilson, D., Charidimou, A. and Werring, D.J., 2014. Advances in understanding spontaneous intracerebral hemorrhage: Insights from neuroimaging. *Expert Rev. Neurother.*, **14**: 661-678. <https://doi.org/10.1586/14737175.2014.918506>
- Yang, Y., Estrada, E.Y., Thompson, J.F., Liu, W. and Rosenberg, G.A., 2007. Matrix metalloproteinase-mediated disruption of tight junction proteins in cerebral vessels is reversed by synthetic matrix metalloproteinase inhibitor in focal ischemia in rat. *J. Cereb. Blood Flow Metab.*, **27**: 697-709. <https://doi.org/10.1038/sj.jcbfm.9600375>
- Wang, G.H., Xiang, J., Lan, R. and Zhang W., 2012. Effect of angong niuhuang pill on neuronal apoptosis and expression of phosphorylated akt in acute ischemic rats. *Chin. Tradit. Pat. Med.*, **34**: 1866-1869.
- Zhang, B.W., Liu, Z.H., 2001. Mechanism of xingnao enema solution in intracerebral hemorrhage absorption and intracranial pressure reduction. *Liaoning J. Tradit. Chin. Med.*, **28**: 571-572.
- Zhang, W.H., Rao, M.L. and Wu, J., 2003. Apoptosis of peripheral tissues of hematoma in experimental intracerebral hemorrhage. *J. Apopl. Nerve Dis.*, **20**: 412-414.
- Zheng, W., Niu, L.J., Zhu, C., Song, S.X., Hou, D.P., Chen, H.Z., Xie, F.M., Zhang, C.P. and Cao, C.G., 2014. Experimental study on the effect of angong niuhuang pill on blood brain barrier and cerebral edema following traumatic brain injury in rats. *Clin. Med. Eng.*, **21**: 1246-1247.
- Zhu, M.X., Dong, H., Lu, Z.H. and Xing, D., 2015. Mechanism of DDR1-MMP9 in the destruction of blood-brain barrier after cerebral ischemic injury in rats. *Chin. J. Neurosurg. Dis. Res.*, **14**: 22-24. <https://doi.org/10.1016/j.neures.2015.01.004>